



## OPEN ACCESS

## EDITED BY

Jerald Thomas,  
University of Wisconsin–Milwaukee,  
United States

## REVIEWED BY

In-Kwon Lee,  
Yonsei University, Republic of Korea  
Sang-Bin Jeon,  
Yonsei University Seoul, Republic of  
Korea, in collaboration with reviewer I-KL  
Evan Suma Rosenberg,  
University of Minnesota Twin Cities,  
United States  
Tongyu Nie,  
University of Minnesota Twin Cities,  
United States, in collaboration with  
reviewer ES

## \*CORRESPONDENCE

Mathieu Lutfallah,  
✉ mlutfallah@ethz.ch

RECEIVED 16 July 2023

ACCEPTED 15 December 2023

PUBLISHED 08 January 2024

## CITATION

Lutfallah M, Ketzel M and Kunz A (2024),  
Redirected walking for exploration of  
unknown environments.  
*Front. Virtual Real.* 4:1259816.  
doi: 10.3389/frvir.2023.1259816

## COPYRIGHT

© 2024 Lutfallah, Ketzel and Kunz. This is  
an open-access article distributed under  
the terms of the [Creative Commons  
Attribution License \(CC BY\)](#). The use,  
distribution or reproduction in other  
forums is permitted, provided the original  
author(s) and the copyright owner(s) are  
credited and that the original publication  
in this journal is cited, in accordance with  
accepted academic practice. No use,  
distribution or reproduction is permitted  
which does not comply with these terms.

# Redirected walking for exploration of unknown environments

Mathieu Lutfallah\*, Marco Ketzel and Andreas Kunz

Innovation Center Virtual Reality, IWF, MAVT, ETH Zurich, Zurich, Switzerland

Real walking is the most natural locomotion method for exploring Virtual Environments (VE), enhancing the immersion of Virtual Reality (VR). Redirected Walking (RDW) is employed to enable real walking within limited tracking spaces in large VEs by subtly manipulating the mapping between the virtual and real environments. However, the effectiveness of RDW is greatly influenced by the convex shape and size of the manually defined physical tracking space, subsequently impacting the user's immersive experience. To improve performance, one strategy is to integrate exploration methods from mobile robotics with RDW. This will expand the usable tracking space, facilitating dynamic environments and rapid exploration. For this, we adapted a Unity framework for an RDW algorithm to facilitate simulations for such an exploration. We conducted a simulation with artificially created non-convex explorable tracking spaces and pre-recorded path elements, simulating two adapted RDW artificial potential field (APF) concepts. Three conceptualized modes were applied: repulsive APF, exploration APF, and exploration APF with a distance threshold. Additionally, one APF was extended with a frontier-based exploration approach that utilized the path between the user's position and a targeted frontier. The analysis revealed a significant trade-off between exploration and immersion. APF combined with frontier-based the exploration technique showed the fastest exploration speed, but - however - resulted in the lowest distance between resets.

## KEYWORDS

virtual reality, locomotion, exploration techniques, redirected walking, redirection

## 1 Introduction

Real walking in virtual environments (VE) has been shown as the most effective navigation technique for achieving high levels of immersion and presence (Usoh et al., 1999). However, utilizing walking to explore virtual worlds imposes limitations on the size of the VE, being constrained by the physical space. Overcoming this restriction can be achieved by altering the mapping between user movements in the VE and the physical environment (PE) described as redirected walking (RDW) (Razzaque et al., 2001). The main target of RDW was initially to steer the user away from boundaries. Some research has tried to employ this method to allow haptic feedback, where the user can be redirected towards objects in the PE that ideally match the same location of the objects in the VE (Thomas et al., 2020). However, it has never been employed to redirect the user to the unknown spaces around them. This aspect is quite important since it could be applied to allow *ad hoc* systems where the user does not need to define the empty space around them. Instead, they could directly run the system and detect the walkable space

while exploring the VE. RDW for exploration also allows the user to continuously update the map of their surroundings and thus have a more arbitrary space.

In RDW, the mapping between the user's movement in the PE and the VE is manipulated. By slightly modifying this mapping, users do not notice these changes since they mainly rely on their visual sense for orientation. The magnitude of such modifications is also named "gain". Several different gains exist to generate a subtle mismatch between the user's visually perceived trajectory and the physical path that he is really walking.

"Rotational gains" indicate the injection of small rotations while the user is standing still or turning on spot. "Translation gains" change the mapping between the linear speed of a user while walking on a straight line, allowing them to either walk slower or faster. "Curvature gains" lead the user to walk along a curved line by injecting rotations into their movement while walking straight. These different alterations of the mapping can be used interchangeably and to a certain extent, meaning the change in mapping is limited to certain thresholds so that the user does neither notice it nor experience any cybersickness. Therefore, many studies have tried to determine these thresholds (Steinicke et al., 2010; Williams and Peck, 2019).

Various steering paradigms have been presented that allow for choosing where the user should be steered to and with what gains. Initial approaches could be distinguished in reactive, scripted, and predicted RDW. Reactive approaches only take into account the current location and orientation of the user in the PE. These methods include techniques such as steer-to-center (S2C) (Razzaque, 2005), where the user is always steered towards the center of the room that is assumed to be convex. In the scripted approach, the walkable paths are predefined, and the gains are also pre-calculated (Azmandian, 2018; Yu et al., 2018). Predictive approaches are the most recent approaches and rely on a prediction of a user's intended path to then apply redirection accordingly. One of the earliest algorithm was RFED (Peck et al., 2012), which describes the paths in walkable corridors by line segments and connecting nodes between them. Taking a user's head orientation into account, the prediction to the next node was calculated. A skeleton graph was also used by Zmuda et al. (Zmuda et al., 2013). The score of a predicted path was then calculated using probabilities assigned to the nodes in this graph. Also MPCRed (Nescher et al., 2014) also used a skeleton graph, but calculates a cost function based on the applied redirections.

Recently, more advanced techniques have been proposed, such as artificial potential fields (APFs), which relax the constraints presented by earlier methods, such as convex and static spaces. With artificial potential fields, it is possible to have a non-convex and dynamic space. Multiuser environments can also be considered in the context of APFs, where multiple users are walking and exploring the VE (Bachmann et al., 2019; Thomas and Rosenberg, 2019). State-of-the-art methods present a new variation of reactive algorithms (Williams et al., 2021a; Williams et al., 2021c; Williams et al., 2022), where the user movement is not predicted, so no computational effort is needed. However, the position and orientation in the VE are also taken into account to enable alignment between the two spaces. A comprehensive overview of existing algorithms is given by Li et al. (2022) and by Nilsson et al. (2018).

So far, RDW algorithms were only applied to redirect the user to avoid collisions with the physical boundaries of the tracking space, but not to guide a user towards yet unknown spaces in the tracking area to explore them further. Thus, the goal of the presented work is the combination of exploration methods from mobile robotics with RDW, as introduced in Lutfallah (2023). Our system dynamically constructs a map based on user movements, and with the inclusion of attractive frontiers, actively directs users to uncharted territories, ensuring a fast exploration. Following a comprehensive map-building phase, users can then transition to other conventional RDW algorithms for further experience refinement.

In this paper the main contributions are the following:

- Design of a simulation framework that would allow testing various RDW algorithms with unknown spaces.
- Development of an exploration logic that can emulate a user walking in large VEs while exploring their surroundings.
- Adaptation of RDW with APF algorithms to allow fast exploration of virtual environments.
- Design of an APF with a frontier base exploration logic that could allow faster exploration of the physical space.

## 2 Related work

### 2.1 Redirected walking in unknown spaces

Nescher et al. (2016) present an approach that combines simultaneous localization and mapping (SLAM) with redirected walking (RDW), allowing free walking in VEs within arbitrary physical environments without the need for a convex dedicated tracking space. In their paper they discuss the use of the Google Tango tablet with MPCRed to have RDW in an unknown space.

An *ad hoc* method for virtual reality systems was presented in the work of Hirt et al. (2017) by allowing the user to map the walls and not having to define the walkable area beforehand. The paper presents a confidence filter that allows going from the point cloud to density on a 2D plan grid. Then - based on the points in the cell - they detect if a cell-area correspond to a wall or not. The Ransac algorithm (Fischler and Bolles, 1981) is then used to find the line and the boundaries. Another work by Hirt et al. (2018b) allows having dynamic objects in the space by creating an occupancy map in the grid.

Another adaptation to support non-convex tracking spaces and multi-user applications is proposed by Thomas and Rosenberg (2019) and Bachmann et al. (2019) by utilizing artificial potential fields originating from the path planning in mobile robotics. The main principle of these RDW methods is to apply a potential within the known tracking space. Hereby, a high potential at the boundaries and obstacles is applied and a low potential in the inner free area of the tracking space. Then, the redirection gains are computed by taking the difference vector between the negative gradient and the previous walking direction at the current user's position. Both showed that their RDW APF algorithms are reliable in non-convex tracking spaces with simulations. However, the tracking spaces were static and predefined, so no extension during the simulation was possible. Li et al. (2022) developed a

taxonomy for RDW and then analyze both, the benefits and shortcomings more in detail.

## 2.2 Exploration in robotics

A lot of research has been put into exploration of unknown spaces in robotics. Although the findings from this research area cannot directly be mapped to RDW, because of humans' walking behavior is less predictable than for robots, some exploration strategies might still be adaptable to RDW. Different approaches have been proposed to allow robots explore unknown spaces in an efficient way. "Topological methods" (Rekleitis et al., 1999) are applied for mobile robots with a limited sensing capability or when metric measurements (e.g., distances, orientation) about the unknown environment are redundant. Hereby, the robot creates a non-directional connectivity graph of its environment. The graph consists of vertices and edges. A vertex represents a unique marker in the surrounding which is placed by the robot. Therefore, an edge represents a closed path between two landmarks. This exploration method is probably not applicable for RDW steering techniques, since the steering algorithms heavily rely on spatial information such as the current user's position. More recently, a hierarchical topology was used for path planning of a robot, which was then combined with a pedestrian model to achieve a safe motion (Han, 2022).

"Gap navigation trees" (Nasir and Elnagar, 2015) are another class of exploration methods. The method's main idea is to enable exploration with a minimal amount of information. Therefore, the algorithm is designed to function with a single sensor which should be capable of detecting gaps in the environment. During the exploration process, a tree structure is then built starting from the initial position. The robot is then guided to these gaps iteratively and new nodes are added to the tree after the gaps were explored. This method could be applicable to RDW, as it saves information such as positions in the nodes and uses them as a target for RDW algorithms such as steer to multiple targets (Hodgson and Bachmann, 2013).

"Potential fields" are also used in mobile robotics for path planning, to avoid collisions with obstacles and also explore unknown environments (Andrews et al., 1983; Khatib, 1986; Prestes et al., 2002). The APF methods in RDW are inspired by this concept. By defining a high potentials at obstacles as well as

starting positions and a low potential at the target positions in a potential function model  $f(x, y)$ , it is possible to navigate a mobile robot by always following the negative gradient vector  $-\nabla f$ . In robotics, it is necessary to avoid local minima in the potential field function. The reason for this is that a robot might become trapped between two local minima, leading to oscillations without ever reaching an external point from which the field would guide it towards a new position. This concern is not present in RDW, owing to the chaotic behavior of the user. Such behavior renders the user's movement non-deterministic; therefore, even if the user is consistently steered to the same minima, they might still move in an opposite direction. This is in contrast to the robot, which strictly follows the gradient. Moreover, past research in mobile robotics and RDW (Thomas and Rosenberg, 2019) has already shown that potential fields work reliably in non-convex tracking spaces. These factors motivated the usage of potential fields for the rest of this work.

"Frontier-based exploration" (Yamauchi, 1997; Gao et al., 2018) is a concept in mobile robotics that involves moving the robot towards the boundary of unknown areas, where the sensor then can register the surrounding and expand the map. This method typically requires the generation of an occupancy grid map. Hereby, the algorithm creates an occupancy grid map consisting of cells which are classified as free, occupied, or unknown. The algorithm then extracts the frontiers and applies possible targets. Subsequently, with the help of the defined reward function, one of these targets is chosen and a path from the current robot's position to the target is computed in the next step. One of the easiest methods to choose a frontier as target is identifying the closest voxel to the robot's current position. The robot is then moved to this place with a path planning algorithm and scans its surrounding. After the frontier is explored, another frontier is chosen based on this cost function and the process repeats until no further frontiers remain.

## 3 Methods

The goal of this work is to adapt RDW for use in unknown spaces. To achieve this, we have developed new algorithms for redirection. In the following section, we will describe the various components required for testing these algorithms, including their development and the setup of the simulation environment. It

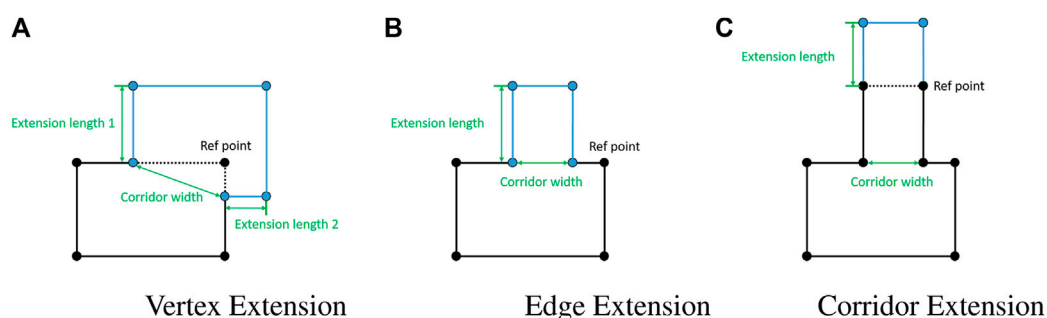


FIGURE 1  
Different types of extensions. (A) Vertex Extension, (B) Edge Extension, (C) Corridor Extension.

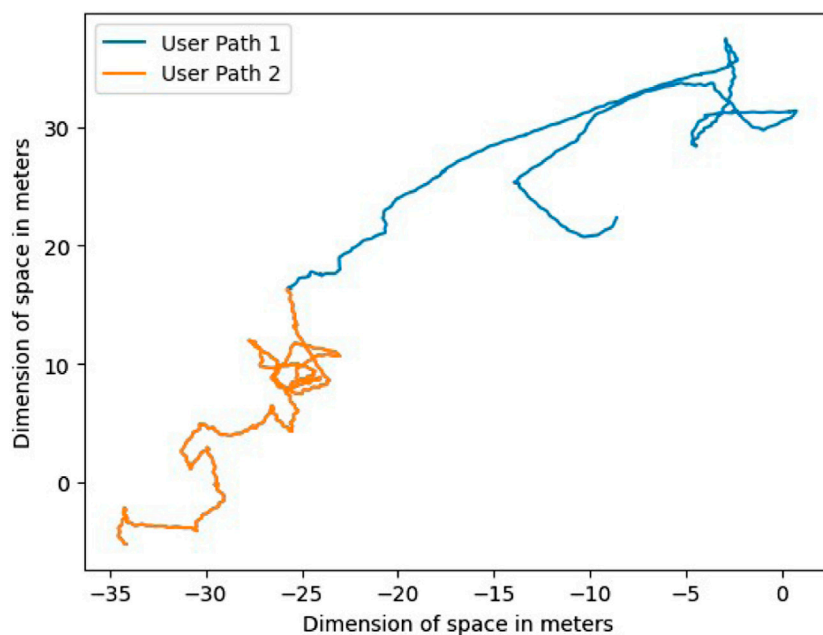


FIGURE 2

New path generated by stitching elements from two other previously recorded real user paths.

should be noted that simulations have been demonstrated to provide a robust platform for evaluating and benchmarking various implementations against one another (Azmandian et al., 2022). As a basis for this work we rely on the OpenRDW framework (Li et al., 2021). This library was extended to generate random, non-convex spaces. Further, an exploration algorithm was developed that allows to progressively expand the map while the user is walking. The implemented APF algorithm was also adapted from that library.

### 3.1 Random room generator

Since the current state of the OpenRDW framework was limited to a set of pre-defined tracking spaces, various arbitrary spaces needed to be created to test our new RDW algorithm for unknown spaces in a simulation and for generalizing the findings. Therefore, a random room generator was implemented. The random room generator started from a small initial room and then gradually extended the tracking space and shape by adding rectangular spaces at different positions of the previous room. Each new rectangular space comes with a center point that will be used later for the exploration strategy as seen in Section 3.5. The size of the initial room was predefined to be a square of  $3 \times 3$  m. Then, the number of extensions was randomly chosen from a uniform distribution. To avoid meaningless extension steps, also the minimum and maximum extension lengths (*MinLength*, *MaxLength*) were defined, as well as the minimum and maximum corridor widths (*MinCorr*, *MaxCorr*) (see Figure 1). By doing so, the size of the new corridor or room was always above a certain size to ensure that the added part contributes a reasonable space. The type of the extension was also randomly chosen from the three types *Vertex Extension*, *Edge Extension*, *Corridor Extension*, as well as the vertex where the extension has to be attached. Three different extensions are

shown in Figure 1. The generator consecutively expanded the room by adding an overlapping extension box to the map. The algorithm is presented in Algorithm 1.

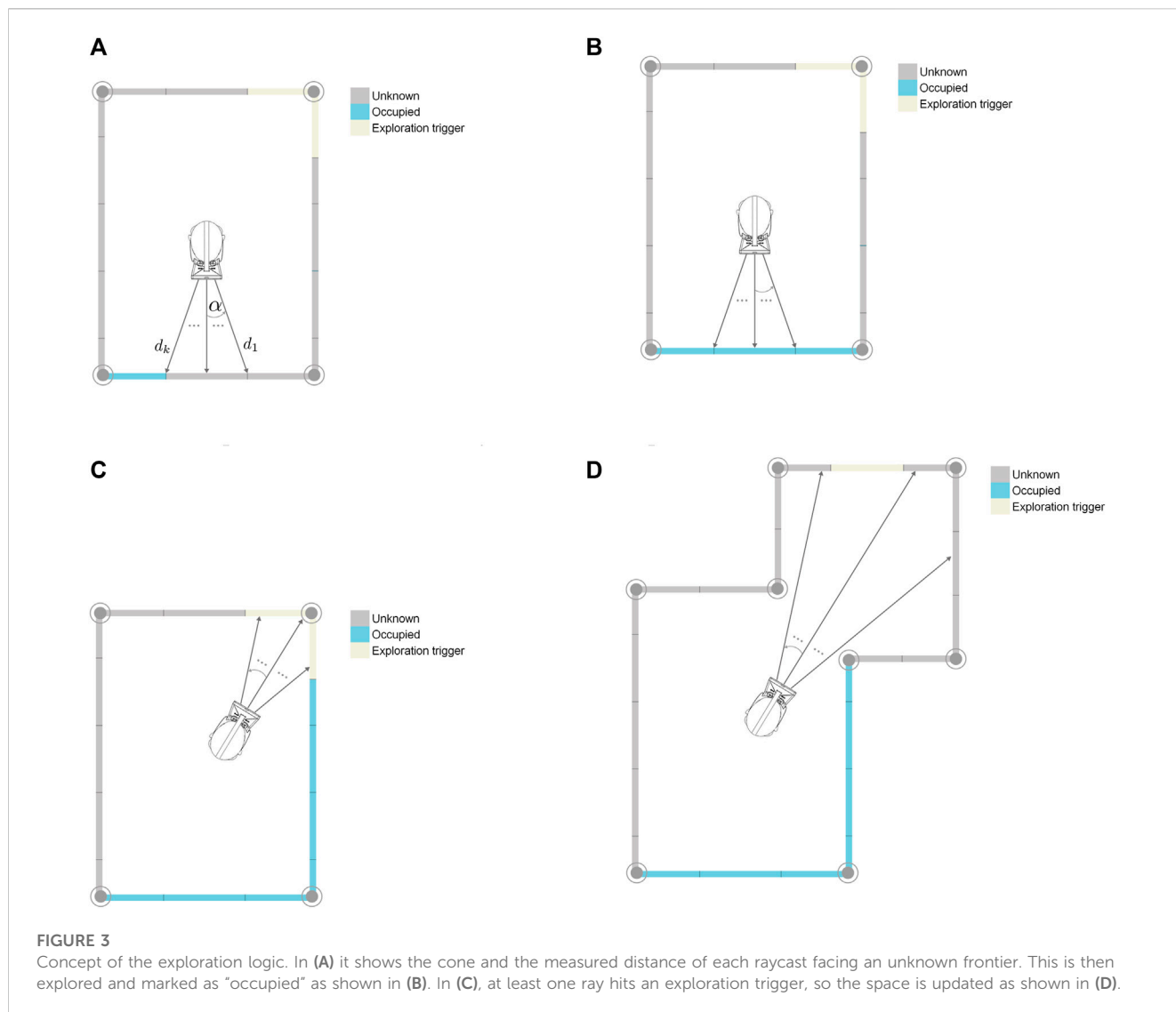
```

1: Define BaseSize
2: for i = 1 to num_extensions do
3:   Randomly choose an extension type and a vertex for
   the extension
4:   Chose vertex where extension is added
5:   if corridor width is within (MinCorr,
   MaxCorr) then
6:     extension_length ← U(MinLength, MaxLength)
7:     Compute remaining points of the extension
8:   end if
9:   Add extension points to the current
   tracking space
10: end for
11: Save all extension points and current tracking space

```

Algorithm 1. Tracking Space Extension Algorithm

The spaces created can then be stored using text files. The starting rectangle vertices are stored. Then the extending points are stored consecutively as well as the center of the newly created box. The center will later on be used for one of the new RDW algorithms. The parameters employed in this study included a base size of 3 m, augmentation with up to 29 extensions, an extension length ranging between 1.0 and 1.2 m, and a corridor width defined between 1.4 and 1.6 m. These values were selected through visual inspection of multiple generated rooms to ensure their practicality and coherence. Additionally, the chosen corridor width was determined to align with typical dimensions observed in residential homes. An example of a generated room is seen in Figure 5.



### 3.2 Path generation

To run our simulations we need a large number of paths. While artificial paths from the “Redirected Walking Toolkit” could be used (Azmandian et al., 2016), this would have resulted in an unnatural faceted walking trajectory. Using real user paths was essential to get reliable results that would translate to real user studies (Hirt et al., 2022). Thus, we used paths from previous studies conducted in the research group. To have a broader data set, we also combined portions of these recorded paths by cutting them and stitching the resulting elements to new paths while adding a certain rotation at the stitching of the parts. This allowed us to have a large number of paths that are later used for the simulations. In Figure 2, a representative stitched path is depicted with two segments merged. For clarity, the image presents only two paths with extended durations to outline their general shapes. For the simulations, segments from paths were selected with a duration of 30 s and were subjected to random rotations ranging from  $-30$  to  $30^\circ$ . Segments continued to be extracted and stitched until the desired

duration was achieved. The specified parameters were determined based on visual analysis of the paths to ensure their appropriateness.

### 3.3 Exploration strategy

As a subsequent step in our implementation, we developed an exploration algorithm designed to continuously update the surrounding map. This ensures that the simulated agent follows previously generated paths, steered by the RDW algorithm, while consistently exploring the boundaries. The mapping process follows the methodology outlined by Hirt et al. (2018a). To simulate the progressive expansion of the map by exploring previously unknown regions, we utilized the simulation environment provided by the OpenRDW library (see Figure 3). We incorporated a cone-shaped ray casting mechanism with the aperture angle  $\alpha$  in the facing direction of the user to detect unknown boundaries in the environment. Initially, the simulation begins with a small exploration map, corresponding to a limited area around the

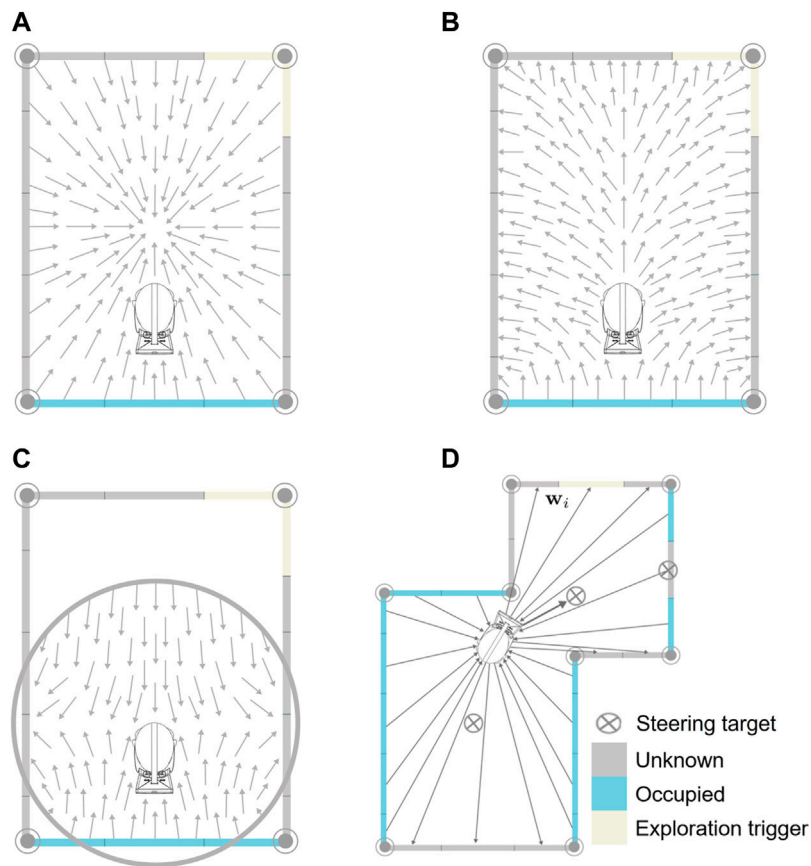


**FIGURE 4**  
The three different modes of APFs. (A) APF mode 1, (B) APF mode 2, (C) APF mode 3, (D) APF mode 4.

**TABLE 1** RDW model parameters applied in the optimization procedure.

Model parameter	Values tested
$\theta_0$	{0.009, 0.018, 0.027}
$\theta_1$	{2.5, 3, 4}
$\theta_2$	{3, 5, 8, 20}

**TABLE 2** Optimal parameter values for modes 1, 2, and 3 with the optimization dataset.

Mode	$\theta_0$	$\theta_1$	$\theta_2$	$\mu_{MapCompleteness}$	$\mu_{DbR}[m]$
1	0.009	4	20	$0.63 \pm 0.10$	$4.78 \pm 1.13$
2	0.009	2.5	20	$0.80 \pm 0.16$	$4.10 \pm 0.87$
3	0.009	2.5	8	$0.77 \pm 0.14$	$4.193 \pm 0.67$

user. The boundaries of the map are classified as initially unknown frontiers. The unknown boundaries are labeled as the “exploration trigger layer” indicating that these frontiers are openings to more expansive spaces. As the user approaches a boundary and the rays intersect with the yet unknown frontier that corresponds to a wall within a distance smaller than the predefined threshold distance  $d_T$ , the frontier is labelled as “occupied”. In case a raycast hits an exploration trigger layer within the distance, the space is extended by the random room generator, then consecutively the new frontiers of the new space are either labeled as unknown boundaries or exploration triggers. The threshold distance  $d_T$  was set to 3 m, which was found to be reliable for SLAM to function effectively with the Google Tango. However, it’s worth noting that the Google Tango is an older device, making this threshold a conservative choice. As for the aperture angle  $\alpha$ , a value of  $55^\circ$  was chosen, providing a field of view of  $110^\circ$ . This decision is

supported by the fact that the camera found in Pico Neo 4 offers a FOV of  $130^\circ$ , and the Intel RealSense camera also has a FOV of  $163^\circ \pm 5^\circ$  for both cameras combined<sup>2</sup>. Since we assume instant detection and extension of the map, a more conservative angle was preferred.

### 3.4 Applied artificial potential field algorithm

Once the simulation framework was established, it allowed for the evaluation of the RDW algorithms. Due to the promising

1 <https://www.picoxr.com/global/products/pico4e/specs>  
2 <https://www.intelrealsense.com/tracking-camera-t265/>



**FIGURE 5**  
Sequential snapshots of a simulation showcasing the user's movement as they progressively explores the environment. The exploration rays are shown in blue.

**TABLE 3 Results of the best performing models on the test dataset.**

Mode	$\mu_{MapCompleteness}$	$\mu_{ExplorationTime}$	$\mu_{ExplorationRate}$	$\mu_{D6R}$
		[s]	[ $min^{-1}$ ]	[m]
1	$0.63 \pm 0.14$	$884 \pm 37.6$	$0.04 \pm 0.01$	$4.80 \pm 1.18$
2	$0.83 \pm 0.12$	$764 \pm 197.1$	$0.07 \pm 0.04$	$4.15 \pm 1.15$
3	$0.79 \pm 0.13$	$780 \pm 199.6$	$0.07 \pm 0.05$	$4.25 \pm 0.91$
4	$0.85 \pm 0.11$	$703.9 \pm 208.6$	$0.08 \pm 0.04$	$3.89 \pm 0.72$

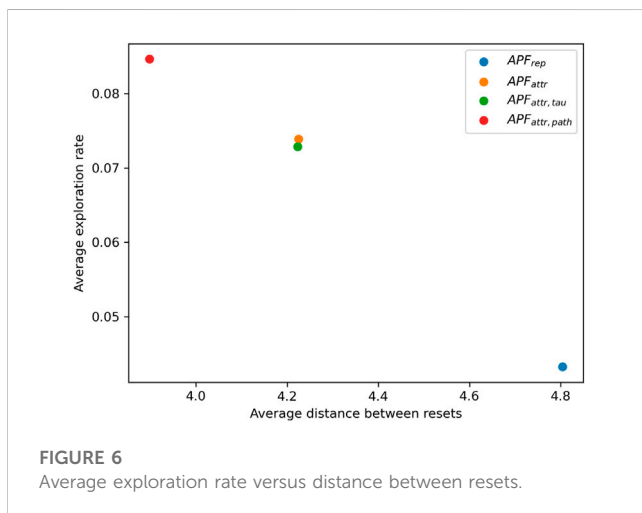


**FIGURE 6**  
Average exploration rate versus distance between resets.

robustness of RDW APF algorithms in non-convex tracking spaces, we decided to adapt chosen RDW models to potential field exploration. The RDW algorithms were implemented based on the main idea of potential field exploration in robotics. Therefore, by applying a high potential on occupied walls and low potentials to frontiers is it possible to redirect the user to unknown areas of interest and enforce exploration. Furthermore, we considered the possible necessity to keep the RDW algorithm versatile. For this purpose, we modeled the RDW APF models with three parameters  $\theta_{0,1,2}$  following the definition by Messinger et al. (2019). As proposed from Bachmann et al. (Bachmann et al., 2019), the redirection vector  $t$  (see Eq. 1) is a sum of individual force vectors. In the initial implementation, the force vector was computed based on the field coming from users as well as boundaries. However, since we are not considering a multi-user application, we only keep the component coming from boundaries.

$$t = \sum_{i=0}^{n_s} w_i(x) \quad (1)$$

Hereby,  $w_i$  is a force associated with segment  $i$  of a boundary with in total of  $n_s$  segments and depending on the current user position  $x$ . The force vector used in this work is shown in Eq. 2.

$$w_i = \begin{cases} \delta_i \cdot \theta_0 \cdot L_i \cdot \frac{e_{d_i}}{|d_i|^{\theta_1}} & \text{if } n \cdot e_{d_i} \geq 0 \text{ and } |d_i| < \theta_2, \\ 0, & \text{otherwise.} \end{cases} \quad (2)$$

The parameters are defined as follows:

- $\delta$  specifies the nature of the boundary force: a value of 1 corresponds to a repulsive force, while a value of  $-1$  indicates an attractive force
- $\theta_0$  is the maximum potential
- $\theta_1$  is the slope distance of the potential base function
- $\theta_2$  distance threshold between the user and the wall
- $L_i$  is the length of the boundary
- $d_i$  is the Euclidean distance between the center of the boundary segment and the current user position
- $e_{d_i}$  is the difference unit vector between this segment center  $i$  and the user's position
- $n$  represents a unit-length vector perpendicular to the boundary, pointing towards the side that faces the tracking area.

Based on the equation we derived, there are three different modes of APF. An illustration of these modes is shown in Figure 4.

1. Repulsive APF: In this mode, only a repulsive field is available, which matches the previous implementation. This means that both unknown frontiers and walls have a  $\delta = 1$ . This will be referred to as mode 1 or  $APF_{rep}$ .

2. Repulsive and Attractive APF: The second mode introduces both repulsive and attractive fields. Here, the unknown frontiers present an attractive field with a  $\delta = -1$ . This will be referred to as mode 2 or  $APF_{att}$ .
3. Repulsive and Attractive APF with limited boundary and frontier effects: In the third mode, the effect of boundaries is limited to only nearby ones, and the same goes for frontiers. This will be referred to as mode 3 or  $APF_{att,r}$ .

Once the total force vector was determined by summing the different individual repulsive and attractive vectors, the gains needed to be applied for the user were computed based on the method developed in the OpenRDW library.

### 3.5 Artificial potential fields with path planning

The previously described modes of APF exhibit certain limitations. One limitation occurs when the environment contains narrow corridors, as the repulsive field generated by the walls consistently directs the user away from the entrance to these corridors. Furthermore, in situations where a user is located in a room that is distant from another room with unexplored boundaries, the APF fails to provide any guidance towards that distant room. Even when utilizing APF mode 2 (the mode without a distance threshold), a decay factor arises due to the inverse relationship with the distance  $d_i$ , which implies that the impact of a more distant frontier or wall is reduced. Another limitation arises when an attractive frontier lacks a direct path, necessitating the user to be steered towards multiple waypoints before reaching the frontier. Consequently, to address these limitations, the APF method was combined with frontier-based exploration.

In this approach, a frontier can be selected in space based on a cost function, which incorporates factors such as distance from the user, length of the unknown frontier, and direction. Initially, we assumed that the user would be redirected towards the furthest frontier until reaching it, as seen in Eq. 3. Once the frontier was chosen, a path planning algorithm was employed to determine the shortest path for the user to reach that frontier. As mentioned earlier in the generation of the spaces, the centers of the created rectangles were stored. Subsequently, the paths were sampled by considering the centers of all the rectangles within the explored area. The goal was to find the path with the shortest distance from the user's starting position to the frontier. The closest center was then selected as the next target point to steer the user towards.

$$P_j^* = \arg \max_{j \in \text{frontiers}} |d_j| \quad (3)$$

where  $P_j^*$  is frontier where the user should be steered and  $d_j$  is the distance between the user and the different frontiers.

Direct steering towards multiple targets has been demonstrated to be less effective than other techniques (Hodgson and Bachmann, 2013). This led us to presenting a novel S2MT algorithm that can be combined with APF (seen in Figure 4D). This approach involved applying an attractive field to a specific target, which was added to the repulsive field generated by the walls. This combination was designed to prevent the user from becoming stuck and encourage

continuous movement away from boundaries. Thus the total force vector on the user can be calculated by Eq. 4. This will be referred to as mode 4 or  $APF_{att, path}$ .

$$t = \sum_{i=0}^n w_i(x; \phi; \theta_0; \theta_1; \theta_2) + \alpha v(x; x_{k+1}) \quad \text{with} \quad \overline{x_k x_{k+1}} \cdot \overline{x_k x} > 0 \quad (4)$$

where the attraction vector  $v(x, x_{k+1})$  from the closest target point  $x_{k+1}$  to the user position  $x$  is defined by Eq. 5 seen below:

$$v = \begin{cases} -\theta_3 \cdot \frac{e_d}{|d|^{\theta_4}} & \text{if } |d| \leq \theta_5 \\ 0 & \text{otherwise} \end{cases} \quad (5)$$

The presented equation resembles Eq. 2, with the exception that it omits the parameters  $L$  and  $\delta$ . This omission is due to the fact that the target point is inherently attractive and lacks a defined length. The parameters  $\theta_3$ ,  $\theta_4$ , and  $\theta_5$  are analogous to  $\theta_0$ ,  $\theta_1$ , and  $\theta_2$  respectively. These were renamed to emphasize that they might have different values, differentiating the properties of the force vector originating from the boundaries from the one related to the steering point. Nevertheless, for the scope of this study, identical values are adopted for both parameter sets.

### 3.6 Parameter fitting

As previously described, the APF function used in this work has three different parameters  $\theta_{0,1,2}$  which are not specified. Previous papers relied on pilot studies to determine these parameters. In this work, we opted for an optimization procedure. For that, 45 tracking spaces were generated with 20 different paths using the random room generator and path generation method previously described. Each tracking space was tested with a combination of four different paths. The parameters were fitted to allow the fastest exploration speed. This was measured using different parameters. Map completeness was used as defined by Yan et al. (2015) which is defined by the ratio of the area of the explored rectangles to the total area of all rectangles constituting our space. We also took into account the exploration time which is defined by the time needed to reach 90% map completeness. Since there was not guarantee that we would reach 90% map completeness we also introduced a metric called "exploration rate" which is the ratio between map completeness and the time. For practical usage, the "map completeness" can measure how well a physical tracking space can be used by a VR application using our new RDW algorithm.

Following the previously described procedure, the best parameters were identified and used for the testing phase where we used 60 different generated tracking spaces in combination with 24 different user paths. Each tracking space was again tested with four different paths.

To find the best model parameters, we followed a grid search approach. Each mode of APF was simulated with a different set of parameters in the optimization set. The parameters tested are shown in Table 1. The parameters chosen were initially derived from the research of previous investigators Messinger et al. (2019); Bachmann et al. (2019). For  $\theta_2$ , this parameter determines the maximum distance between the user and the walls beyond which forces are



no longer exerted. This effectively limits the rooms that can influence the user, so values for  $\theta_2$  were chosen with this in mind. A preliminary evaluation of all the parameters was conducted by testing various ones in a few rooms to identify which required further investigation. In future studies, we plan to conduct a comprehensive exploration across a broader range of parameters.

### 3.7 Simulation conditions

For all the simulations, various parameters had to be defined. First the reset algorithm employed in all of the simulation is based on APF-R proposed by Bachmann et al. (2019). After the potential field at the position of the user is computed, the user is rotated to face toward that vector and the simulation continues. The translation speed used in the simulation is set to 1 m/s and the rotation speed to 90°. This is inline with previous studies (Williams et al., 2021b; Williams et al., 2021c). The reset is triggered when the user is 0.3 m away from boundaries. The redirection gain thresholds employed in both optimization and testing are based on the work of Steinicke et al. (2010) and is widely used by researchers (Bachmann et al., 2019; Williams et al., 2021c). The translation gain is bounded to be between 0.86 and 1.26, the rotational gain between 0.67 and 1.24, and the curvature gain between -7.5 and 7.5.

## 4 Results

The best simulation results based on the mean map completeness are shown in Table 2. The APF combined with the frontier based method (mode 4) was not trained under the assumption that the same parameter from mode 2 should be applicable since the same APF baseline is used. Additionally example images from a simulation are shown in Figure 5.

Table 3 shows the results on the simulations with the test data from the second dataset. Furthermore, it lists the mean values of MapCompleteness, ExplorationTime, ExplorationRate, and Distance between Resets (DbR) together with their standard deviation. Additionally, it shows the test results from the model combined with the frontier based exploration (Mode 4).

When comparing the results from the modes 1, 2 and 3 between the optimization and test datasets, it is noticeable that the mean values are quite similar. The standard deviation of the simulations with the test dataset regarding the DbR is slightly higher. Therefore, it can be assumed that the parameter fitted are adaptable to unknown tracking spaces, regardless of the mode.

From the results it is clear that a trade-off exists between exploration rate and DbR. This is further seen in Figure 6. Having attractive fields lead to higher average exploration rate but lower average DbR compared to having only repulsive forces. Furthermore, it seems to be that the repulsive APF does not discover the whole tracking space within the time window. This is clearly visible in the ExplorationTime whose average is about the maximum simulation time of 900s and the MapCompleteness with the small standard deviation. In opposite to this, the APFs with mode 2-3 often reached the threshold of 90% map completeness. Therefore, as expected, adding an attractive component to unknown

boundaries led to faster exploration, meaning that the user utilizes the available tracking space more quickly. The exploration APF with the frontier based exploration (mode 4) shows the highest mean values regarding the exploration. This indicates that the additional attraction to a computed path to a frontier works as expected and facilitates the redirection of the user to unknown areas of the tracking space. On the other hand, mode 4 has the lowest DbR. Therefore, the expected additional redirection to open spaces led to more resets.

We could not find a normal distribution in our results based on the Shapiro-Wilk test. A significance level of 5% was employed. We compared the three APF modes that included an attractive component (modes 2, 3, and 4) to mode 1, which only consisted of a repulsive field, regarding different metrics.

In terms of map completeness, we began by applying a Kruskal-Wallis test among the different modes. This yielded a  $p$ -value of  $2.96 \times 10^{-13}$ , indicating that there is a significant difference between the groups. To further investigate the pairs, we employed the Mann-Whitney U test with a Bonferroni correction to prevent occurrences of type 1 error, given that we are conducting multiple successive comparisons. As we have 3 tests, the new significance level becomes  $\frac{5\%}{3} \approx 1.67\%$ . Assuming that modes 2, 3, and 4 have a higher map completeness time compared to mode 1, we obtained the following  $p$ -values using the Mann-Whitney U test:

- Mode 2 vs. Mode 1:  $p = 1.93 \times 10^{-10}$  (CL: 0.8663),
- Mode 3 vs. Mode 1:  $p = 2.88 \times 10^{-7}$  (CL: 0.7928),
- Mode 4 vs. Mode 1:  $p = 4.16 \times 10^{-12}$  (CL: 0.8996).

This confirms that a statistically significant difference exists between the distributions, supporting the previous hypothesis that the attractive component of the algorithms aided in exploration. We also compared modes 2 and 3 with 4 in terms of map completeness. However, the  $p$ -values were significantly higher than the corrected significance level, adjusted for multiple comparisons. This suggests that further investigation is needed to support the hypothesis that combining the APF with a frontier-based approach allows for a more thorough exploration of the environment.

In terms of DbR, we again first conducted the Kruskal-Wallis test where we found  $p = 1.73 \times 10^{-3}$  signaling a significant difference between the modes. Thus we conducted a Mann-Whitney U rank test with the Bonferroni correction comparing modes 2, 3, and 4 to mode 1, which had no attractive component. The results were as follows:

- Mode 2 vs. Mode 1:  $p = 0.006$  (CL: 0.6460),
- Mode 3 vs. Mode 1:  $p = 0.009$  (CL: 0.6389),
- Mode 4 vs. Mode 1:  $p = 1.04 \times 10^{-4}$  (CL: 0.7176).

The Null hypotheses of all comparisons with  $APF_{rep}$  were rejected due to  $p < 1.67\%$ , suggesting the performance regarding the DbR of  $APF_{rep}$  is significantly higher than an APF with attractive components. It follows that applying attraction fields to facilitate exploration can remarkably decrease DbR, thus accelerating exploration of the tracking space. Comparisons between modes 2, 3, and 4 yielded  $p$ -values higher than the further more corrected significance level, implying the Null hypothesis could not be

rejected. Further investigation would be necessary to validate the hypothesis that combining the APF with a frontier-based exploration can lead to a smaller average distance between resets, compared to the other two modes that included attractive components.

We can conclude that the use of attractive forces to guide users towards unknown areas leads to faster exploration; however, this results in more resets. This outcome was anticipated and has been validated in this study. It presents an opportunity to investigate the trade-off between rapid exploration and optimal user experience, where users encounter less resets. This suggests that a stopping criterion could be implemented to eliminate the need for exploration and switch to already-developed algorithms. Another intriguing question is whether faster exploration could lead to a quicker transition to existing algorithms, potentially enhancing the overall user experience due to a reduced transition phase. We hope this study paves the way for research in these two emerging fields.

## 4.1 Limitations

The following work is based on simulations; therefore, further real user studies are necessary to validate the results (Hirt et al., 2022). However, this work presents an initial starting point, providing methods that could be employed to utilize RDW in unknown spaces. There are certain differences between the simulations and the real world. Firstly, the simulations utilize a discrete exploration of the spaces. As mentioned earlier, a new section is added to the map after each exploration, albeit small due to the overlap of the rectangles. This discrete exploration approach contrasts with the continuous exploration scheme typically found in the real world.

The second limitation of our methods lies in the absence of any errors in the mapping algorithm, which does not reflect the reality of a real-world scenario. Additionally, the spaces in our simulations are static, assuming no changes occur to previously explored sections. However, this assumption may not hold in the real world, where objects can be moved. Moreover, despite utilizing real user study trajectories, these may introduce biases in terms of what actual users would do in a practical environment.

Another limitation is that current commercial standalone head-mounted displays (HMDs) do not provide access to the point cloud they produce for tracking. Consequently, a special license would be required to extract this point cloud, which is essential for identifying the empty spaces around the user. An alternative solution might involve using an external camera, but this addition could introduce overhead into the system. It's crucial to highlight that all algorithm configurations tested in this study operate in real-time. However, tests showcasing this real-time capability did not include the component that converts the point cloud into a 2D map representing the empty spaces.

## 5 Conclusion

This study aimed to adapt a previously established RDW algorithms to the exploration of unknown physical spaces. To achieve this, we developed a simulation framework capable of creating random spaces and subsequent exploration. We tested

four different alterations of the APF RDW algorithm to assess their effectiveness in facilitating exploration.

The first mode of the APF RDW algorithm included repulsive fields from both walls and unknown boundaries. The second variation incorporated repulsive fields from walls and an attractive field towards unknown boundaries. The third variation was similar to the second, but it completely removed the effect from faraway boundaries. Lastly, we combined the second variation with a frontier-based exploration approach, guiding the user towards multiple intermediate targets determined by a path planning algorithm, where the final goal is to reach a far way frontier in the space.

Using the simulation framework, we conducted an optimization phase to determine the best model parameters for each APF mode. Subsequently, a testing round was performed to evaluate their performance. Our main finding indicates that including an attractive component towards unknown boundaries can lead to faster exploration of the virtual space. However, this approach also resulted in a lower average DbR.

While efforts were made to enhance the realism of the simulations, certain limitations remain. The discrete nature of space exploration within the simulation and uncertainties regarding the generalization of the selected paths to real-world experiments pose potential challenges. Future research should address these limitations to further refine the redirected walking algorithm and ensure its applicability in practical scenarios.

In summary, this work contributes to the understanding of how different alterations of the APF RDW algorithm can impact the exploration of new virtual spaces. By incorporating an attractive component towards unknown boundaries, faster exploration is achievable, albeit with an increased frequency of resets. These findings provide valuable insights for researchers and developers working on improving redirected walking techniques, ultimately enhancing user experiences in virtual reality applications.

## 6 Future work

In future work, several potential directions and improvements can be explored to enhance the algorithm's performance and extend its applicability in various scenarios. A next step which might improve the results of the algorithm is to apply unsymmetrical forces to frontiers and walls. This can be done by adjusting the parameter. Applying a smaller beta would mean that the attraction fields to frontiers are weaker, resulting in an increased DbR. Another interesting aspect could be to construct this concept dynamically over time. For example, the value could be large in the beginning to accelerate the exploration and then lowered to adjust the DbR. Moreover, we could totally stop the attraction field at a certain point where the map is satisfying. Thus a stopping criteria need to be explored.

For future research, looking into the effect of the shape and size of the tracking space could be also interesting. It might be worth to investigate the conditions of a tracking space when a repulsive and explorative algorithm do not significantly differ from each other. Based on this, a decision-making could be embedded which could decide if a tracking space should be extended or not by considering the shape and/or the size of the tracking space. Furthermore, more pertinent metrics and enhanced visualization tools, like heatmaps, would be essential for evaluating different algorithms.

To approve the simulation results, the algorithms could be embedded in the framework on a setup with real walking. Then, they can be tested and the data logged to check if simulation results and real results are similar. Another interesting aspect for future work will be a multi-user setup. In a multi-user setup to determine whether it is possible to better utilize the available tracking space in the same time.

## Data availability statement

The raw data supporting the conclusion of this article will be made available by the authors, without undue reservation.

## Author contributions

ML: Conceptualization, Supervision, Writing—original draft, Writing—review and editing. MK: Data curation, Formal Analysis, Investigation, Software, Writing—original draft. AK: Conceptualization, Methodology, Project administration, Supervision, Validation, Writing—review and editing.

## References

- Andrews, J. R., and Hogan, N. (1983). *Impedance control as a framework for implementing obstacle avoidance in a manipulator*. Dept. of Mechanical Engineering. Master's thesis, M. I. T.
- Azmandian, M. (2018). *Design and evaluation of adaptive redirected walking systems*. University of Southern California. Ph.D. thesis.
- Azmandian, M., Grechkin, T., Bolas, M., and Suma, E. (2016). "The redirected walking toolkit: a unified development platform for exploring large virtual environments," in 2016 IEEE 2nd Workshop on Everyday Virtual Reality (WEVR), 9–14. doi:10.1109/WEVR.2016.7859537
- Azmandian, M., Yahata, R., Grechkin, T., Thomas, J., and Rosenberg, E. S. (2022). Validating simulation-based evaluation of redirected walking systems. *IEEE Trans. Vis. Comput. Graph.* 28, 2288–2298. doi:10.1109/TVCG.2022.3150466
- Bachmann, E. R., Hodgson, E., Hoffbauer, C., and Messinger, J. (2019). Multi-user redirected walking and resetting using artificial potential fields. *IEEE Trans. Vis. Comput. Graph.* 25, 2022–2031. doi:10.1109/TVCG.2019.2898764
- Fischler, M. A., and Bolles, R. C. (1981). Random sample consensus: a paradigm for model fitting with applications to image analysis and automated cartography. *Commun. ACM* 24, 381–395. doi:10.1145/358669.358692
- Gao, W., Booker, M., Adiwahono, A., Yuan, M., Wang, J., and Yun, Y. W. (2018). "An improved frontier-based approach for autonomous exploration," in 2018 15th International Conference on Control (Automation, Robotics and Vision (ICARCV)), 292–297. doi:10.1109/ICARCV.2018.8581245
- Han, J.-w. (2022). *Safe and efficient navigation of a mobile robot: path planning based on hierarchical topology map and motion planning with pedestrian behavior model*. Ph.D. thesis, University of Waterloo.
- Hirt, C., Kompis, Y., Holz, C., and Kunz, A. (2022). "The chaotic behavior of redirection—revisiting simulations in redirected walking," in 2022 IEEE Conference on Virtual Reality and 3D User Interfaces (VR) (IEEE), 524–533.
- Hirt, C., Zank, M., and Kunz, A. (2017). "Real-time wall outline extraction for redirected walking," in Proceedings of the 23rd ACM Symposium on Virtual Reality Software and Technology (ACM), 72.
- Hirt, C., Zank, M., and Kunz, A. (2018a). "Geometry extraction for *ad hoc* redirected walking using a slam device," in International Conference on Augmented Reality, Virtual Reality and Computer Graphics (Springer), 35–53.
- Hirt, C., Zank, M., and Kunz, A. (2018b). "Preliminary environment mapping for redirected walking," in 25th IEEE Conference on Virtual Reality and 3D User Interfaces (IEEE VR 2018) (IEEE), 573–574.
- Hodgson, E., and Bachmann, E. (2013). Comparing four approaches to generalized redirected walking: simulation and live user data. *IEEE Trans. Vis. Comput. Graph.* 19, 634–643. doi:10.1109/TVCG.2013.28
- Khatib, O. (1986). Real-time obstacle avoidance for manipulators and mobile robots. *Int. J. robotics Res.* 5, 90–98. doi:10.1177/027836498600500106
- Li, Y.-J., Steinicke, F., and Wang, M. (2022). A comprehensive review of redirected walking techniques: taxonomy, methods, and future directions. *J. Comput. Sci. Technol.* 37, 561–583. doi:10.1007/s11390-022-2266-7
- Li, Y.-J., Wang, M., Steinicke, F., and Zhao, Q. (2021). "Openrdw: a redirected walking library and benchmark with multi-user, learning-based functionalities and state-of-the-art algorithms," in 2021 IEEE International Symposium on Mixed and Augmented Reality (ISMAR), 21–30. doi:10.1109/ISMAR52148.2021.00016
- Lutfallah, M. (2023). "[dc] maximizing natural walking in virtual environments," in 2023 IEEE Conference on Virtual Reality and 3D User Interfaces Abstracts and Workshops (VRW) (IEEE), 989–990.
- Messinger, J., Hodgson, E., and Bachmann, E. R. (2019). "Effects of tracking area shape and size on artificial potential field redirected walking," in 2019 IEEE Conference on Virtual Reality and 3D User Interfaces (VR), 72–80. doi:10.1109/VR.2019.8797818
- Nasir, R., and Elnagar, A. (2015). Gap navigation trees for discovering unknown environments. *Intelligent Control Automation* 06, 229–240. doi:10.4236/ica.2015.64022
- Nescher, T., Huang, Y.-Y., and Kunz, A. (2014). "Planning redirection techniques for optimal free walking experience using model predictive control," in 2014 IEEE Symposium on (IEEE), 111–118. 3D User Interfaces (3DUI).
- Nescher, T., Zank, M., and Kunz, A. (2016). "Simultaneous mapping and redirected walking for *ad hoc* free walking in virtual environments," in 2016 IEEE Virtual Reality (VR), 239–240. doi:10.1109/VR.2016.7504742
- Nilsson, N. C., Peck, T., Bruder, G., Hodgson, E., Serafin, S., Whitton, M., et al. (2018). 15 years of research on redirected walking in immersive virtual environments. *IEEE Comput. Graph. Appl.* 38, 44–56. doi:10.1109/mcg.2018.111125628
- Peck, T. C., Fuchs, H., and Whitton, M. C. (2012). The design and evaluation of a large-scale real-walking locomotion interface. *IEEE Trans. Vis. Comput. Graph.* 18, 1053–1067. doi:10.1109/tvcg.2011.289
- Prestes, E., Engel, P., Trevisan, M., and Idiart, M. (2002). Exploration method using harmonic functions. *Robotics Aut. Syst.* 40, 25–42. doi:10.1016/S0921-8890(02)00209-9
- Razzaque, S. (2005). *Redirected walking*. University of North Carolina at Chapel Hill.
- Razzaque, S., Kohn, Z., and Whitton, M. C. (2001). Redirected walking. *Proc. Eurogr. Manch. UK* 9, 105–106.
- Rekleitis, I., Dujmovic, V., and Dudek, G. (1999). "Efficient topological exploration," in Proceedings 1999 IEEE International Conference on Robotics and Automation (Cat. No.99CH36288C) 1, 676–681. doi:10.1109/ROBOT.1999.770053
- Steinicke, F., Bruder, G., Jerald, J., Frenz, H., and Lappe, M. (2010). Estimation of detection thresholds for redirected walking techniques. *IEEE Trans. Vis. Comput. Graph.* 16, 17–27. doi:10.1109/tvcg.2009.62
- Thomas, J., Hutton Pospick, C., and Suma Rosenberg, E. (2020). "Towards physically interactive virtual environments: reactive alignment with redirected walking," in VRST

## Funding

The author(s) declare financial support was received for the research, authorship, and/or publication of this article. Open access funding by ETH Zurich.

## Conflict of interest

The authors declare that the research was conducted in the absence of any commercial or financial relationships that could be construed as a potential conflict of interest.

## Publisher's note

All claims expressed in this article are solely those of the authors and do not necessarily represent those of their affiliated organizations, or those of the publisher, the editors and the reviewers. Any product that may be evaluated in this article, or claim that may be made by its manufacturer, is not guaranteed or endorsed by the publisher.

'20 Proceedings of the 26th ACM Symposium on Virtual Reality Software and Technology (New York, NY, USA: Association for Computing Machinery), 1–10. doi:10.1145/3385956.3418966

Thomas, J., and Rosenberg, E. S. (2019). "A general reactive algorithm for redirected walking using artificial potential functions," in 2019 IEEE Conference on Virtual Reality and 3D User Interfaces (VR) (IEEE), 56–62.

Usoh, M., Arthur, K., Whitton, M. C., Bastos, R., Steed, A., Slater, M., et al. (1999). "Walking walking-in-place flying, in virtual environments," in SIGGRAPH '99 Proceedings of the 26th Annual Conference on Computer Graphics and Interactive Techniques (USA: ACM Press/Addison-Wesley Publishing Co.), 359–364. doi:10.1145/311535.311589

Williams, N. L., Bera, A., and Manocha, D. (2021a). ARC: alignment-based redirection controller for redirected walking in complex environments. *IEEE Trans. Vis. Comput. Graph.* 27, 2535–2544. doi:10.1109/tvcg.2021.3067781

Williams, N. L., Bera, A., and Manocha, D. (2021b). ARC: alignment-based redirection controller for redirected walking in complex environments. *CoRR abs/2101.04912*

Williams, N. L., Bera, A., and Manocha, D. (2021c). Redirected walking in static and dynamic scenes using visibility polygons. *IEEE Trans. Vis. Comput. Graph.* 27, 4267–4277. doi:10.1109/TVCG.2021.3106432

Williams, N. L., Bera, A., and Manocha, D. (2022). "Eni: quantifying environment compatibility for natural walking in virtual reality," in 2022 IEEE Conference on Virtual Reality and 3D User Interfaces (VR) (IEEE), 419–427.

Williams, N. L., and Peck, T. C. (2019). Estimation of rotation gain thresholds considering fov, gender, and distractors. *IEEE Trans. Vis. Comput. Graph.* 25, 3158–3168. doi:10.1109/TVCG.2019.2932213

Yamauchi, B. (1997). "A frontier-based approach for autonomous exploration," in Proceedings 1997 IEEE International Symposium on Computational Intelligence in Robotics and Automation CIRA'97, 146–151. "Towards New Computational Principles for Robotics and Automation". doi:10.1109/CIRA.1997.613851

Yan, Z., Fabresse, L., Laval, J., and Bouraqadi, N. (2015). "Metrics for performance benchmarking of multi-robot exploration," in 2015 IEEE/RSJ International Conference on Intelligent Robots and Systems (IROS), 3407–3414. doi:10.1109/IROS.2015.7353852

Yu, R., Duer, Z., Ogle, T., Bowman, D. A., Tucker, T., Hicks, D., et al. (2018). "Experiencing an invisible world war i battlefield through narrative-driven redirected walking in virtual reality," in 2018 IEEE Conference on Virtual Reality and 3D User Interfaces (VR) (IEEE), 313–319. doi:10.1109/vr.2018.8448288

Zmuda, M. A., Wonsler, J. L., Bachmann, E. R., and Hodgson, E. (2013). Optimizing constrained-environment redirected walking instructions using search techniques. *IEEE Trans. Vis. Comput. Graph.* 19, 1872–1884. doi:10.1109/tvcg.2013.88